Research Article

Journal of Physical Organic Chemistry

Received: 23 January 2008, Revised: 7 April 2008, Accepted: 8 April 2008, Published online in Wiley InterScience: 2008

(www.interscience.wiley.com) DOI 10.1002/poc.1389

Impact of intermolecular hydrogen bond on structural properties of phenylboronic acid: quantum chemical and X-ray study

Michał K. Cyrański[a], Aneta Jezierska[b], Paulina Klimentowska[a], Jarosław J. Panek[c] and Andrzej Sporzyński[d]*

The molecular structure and properties of phenylboronic acid were investigated experimentally using X-ray structural analysis and spectroscopic methods. Infrared (IR) spectroscopy measurements were performed to assess the hydrogen bonding strength. The experimental part is enhanced by computational results concerning the geometrical and electronic structure. The molecular dimer (basic structural motif) was investigated on the basis of density functional theory (DFT) and Møller–Plesset second order (MP2) perturbation theory. The basis-set superposition error (BSSE) was calculated to correct the binding energy. Atoms in molecules (AIM) and topological analysis of electron localization function (ELF) were applied to study the intermolecular hydrogen bond properties and localization pattern for the neighborhood of the boron atom. The anharmonicity of the hydrogen bond potential function was studied by solving the time-independent Schrödinger equation. Potential energy distribution (PED) analysis of the normal modes was performed to identify the characteristic frequencies of the studied system. Subsequently, the interaction energy for the dimeric form was decomposed using the symmetry-adapted perturbation theory (SAPT) scheme. Car–Parrinello molecular dynamics (CPMD) gave an insight into dynamical processes occurring in the phenylboronic acid dimer *in vacuo*. The hydrogen bridge protons in the phenylboronic acid are not shifted significantly toward the acceptor. Lower dimerization energy with respect to the carboxylic acid dimers is explained on the basis of the interaction energy decomposition as the effect of diminished induction term. The employment of SAPT and CPMD approaches is a step forward in the understanding of the physico-chemical nature of the large family represented by the investigated compound. Copyright © 2008 John Wiley & Sons, Ltd.

Supplementary electronic material for this paper is available in Wiley InterScience at http://www.mrw.interscience.wiley.com/suppmat/0894-3230/suppmat/

Keywords: phenylboronic acid; hydrogen bond; X-ray structure; DFT; MP2; BSSE; AIM; ELF; PED; SAPT; CPMD

INTRODUCTION

Boronic acids, $RB(OH)_2$, have become an object of recent increasing interest due to their new applications in organic synthesis, catalysis, supramolecular chemistry, biology, medicine,[1] and materials science.[2] This interest is essentially stimulated by their extensive use in organic chemistry as chemical building blocks and/or intermediates. Numerous synthetic routes were developed after Miyaura and Suzuki's discovery of palladium-catalyzed coupling of arylboronic acids with aryl halides.[3] They have also been applied in Petasis synthesis of α-aminoacids.[4] In medicinal chemistry, boronic acids are used in cancer treatment as an ingredient of boron neutron capture therapy (BNCT)[5] or chemotherapeutic agents.[6] Boronic acids are also used as antibiotics[7–9] and enzyme inhibitors.[10–12] Their unique feature of forming reversible covalent complexes with sugars (but also with aminoacids, hydroxamic acids, etc.) has been extensively exploited toward the invention of new saccharide sensors[13,14] particularly focused on the measurement of the blood glucose level of diabetes patients.[15] Following the research on molecular recognition, phenylboronic acids have also recently been employed as promising building blocks in crystal engineering in order to achieve predictably organized crystal materials.[16–20] Supramolecular assemblies of various types have been generated in this manner.[2,16,21–23]

* *Correspondence to: A. Sporzyński, Faculty of Chemistry, Warsaw University of Technology, Noakowskiego 3, 00-664 Warsaw, Poland.*
E-mail: spor@ch.pw.edu.pl

a *M. K. Cyrański, P. Klimentowska*
Faculty of Chemistry, University of Warsaw, Pasteura 1, 02-093 Warsaw, Poland

b *A. Jezierska*
Faculty of Chemistry, University of Wrocław, Joliot-Curie 14, 50-383 Wrocław, Poland

c *J. J. Panek*
National Institute of Chemistry, Hajdrihova 19, 1001 Ljubljana, Slovenia

d *A. Sporzyński*
Faculty of Chemistry, Warsaw University of Technology, Noakowskiego 3, 00-664 Warsaw, Poland

Copyright © 2008 John Wiley & Sons, Ltd.

Arylboronic acids contain a $-B(OH)_2$ functional group. Each of the hydroxyl groups bonded to the boron atom may participate in hydrogen bonds and usually a complex network of hydrogen-bonded molecules is observed in the solid state.[24] Similarly to carboxylic acids, the most common structural motif of phenylboronic acids is a cyclic dimer generated by a pair of intermolecular hydrogen bonds. This subunit is observed in the crystal structure of the archetypal system, phenylboronic acid, the structure of which was reported 30 years ago by Rettig and Trotter,[25] and in most of about 50 arylboronic acids and/or their complexes with known crystal structures.[26]

The crystal structure determination reported by Rettig and Trotter[25] was carried out at room temperature (295 K). However, an increasing number of recently published structures of boronic acids refer to lower temperatures to reduce thermal motions and to provide more accurate structural data useful, for example, in further comparison with additional experimental and theoretical models. Temperature-dependent crystallographic studies allow for locating phase transitions in the solid state. In order to establish a reference system for low temperature conditions, we redetermined the crystal and molecular structure of the phenylboronic acid at 100 K. The new experimental findings are supported by the theoretical investigations on the molecular dimer. Density functional theory (DFT)[27,28] and Møller–Plesset second order (MP2)[29] perturbation theory calculations were used and compared with the previous theoretical results reported by Rodriguez-Cuamatzi *et al.*[19] for the boronic acid derivatives family. The cited study is devoted to the design of highly stable hydrogen-bonded supramolecular system. The interaction energy and geometrical parameters were therefore of primary interest to the authors of Reference [19], while our study is devoted to the detailed description of the molecular properties of phenylboronic acid dimer with particular stress on the electronic structure and dynamical time evolution of selected parameters. To give an insight into the topology of the electron density and intermolecular hydrogen bond properties, the study is supported by the Bader's Atoms in Molecules (AIM) theory.[30] Electron localization function (ELF) revealed the pattern of regions in space connected with localization domains of electrons which was useful for the determination of bonding properties.[31] In addition, the experimental infrared (IR) spectrum of the phenylboronic acid reported by Faniran and Shurvell[32] formed a basis for our further computational investigations involving potential energy distribution (PED) technique[33] and anharmonicity estimation by solving the 1D time-independent Schrödinger equation[34] for the vibrational problem. Subsequently, the theoretical part also describes the interaction energy partitioning by application of the symmetry-adapted perturbation theory (SAPT) scheme proposed by Jeziorski *et al.*[35] Finally, Car–Parrinello molecular dynamics (CPMD) method was employed to study the time evolution of dimeric structure in gas phase on the basis of the DFT potential energy surface (PES).[36] Carboxylic acid dimers have been extensively studied using the CPMD approach.[37,38] Most CPMD studies involving boron are restricted to doped materials investigations.[39,40]

The main aim of the study was the detailed description of the archetypal boronic acid dimer using both experimental and computational techniques. Special attention was paid to the study of interaction energy origins in the dimer and spectroscopic implications of dimerization. Additionally, application of CPMD technique to the boronic acid family is presented.

EXPERIMENTAL AND COMPUTATIONAL METHODOLOGIES

Physicochemical measurements

The X-ray measurement of phenylboronic acid was performed at 100 (2) K on a KUMA CCD *k*-axis diffractometer with graphite-monochromated Mo Kα radiation (0.71073 Å). The crystal was positioned at a distance of 62.25 mm from the KM4CCD camera; 748 frames were measured at 0.8° intervals on a counting time of 30 s. Data reduction and analysis were carried out with the Kuma Diffraction programs. The data were corrected for Lorentz and polarization effects but no absorption correction was applied. The structure was solved by direct methods[41] and refined by using the SHELXL program.[42] The refinement was based on F^2 for all reflections except for those with very negative F^2. The weighted R factor, wR and all goodness-of-fit S values are based on F^2. The non-hydrogen atoms were refined anisotropically. Hydrogen atoms were located from a difference Fourier map; their positions and thermal parameters were refined isotropically. The atomic scattering factors were taken from the International Tables for Crystallography.[43] Data summary: $C_6H_7BO_2$, colorless crystal, $0.3 \times 0.25 \times 0.2\ mm^3$, formula weight $M = 121.93$, orthorhombic, space group Iba2, $a = 15.095\ (3)$ Å, $b = 17.867\ (4)$ Å, $c = 9.729\ (2)$ Å, $V = 2623.9\ (9)$ Å^3, $Z = 16$, $D_x = 1.235\ Mg/m^3$, $F(000) = 1024$, absorption coefficient $\mu = 0.18\ mm^{-1}$. The collected data range was $3.53 < \Theta < 24.99°$ ($-17 \le h \le 17$, $-21 \le k \le 21$, $-11 \le l \le 9$), 9627 reflections collected, 1897 [R(int) = 0.0405] unique reflections, goodness-of-fit on $F^2 = 0.998$, final $R = 0.0286$, w$R^2 = 0.0597$ [for all 1676 $F_0 > 4\ \sigma(F_0)$], $R = 0.0342$, w$R^2 = 0.0621$ (for all data), weight $= 1/[\sigma^2(F_0^2) + (0.0357P)^2 + 0.00P]$ where $P = (F_0^2 + 2\ F_c^2)/3$, extinction coefficient = 0.0025(4), maximum and minimum difference electron densities were 0.150 and $-0.134\ e \cdot Å^{-3}$. Crystallographic data for the structure has been deposited with the Cambridge Crystallographic Data Centre as supplementary publication No. CCDC 654342. Copies of the data can be obtained on application to CCDC, 12 Union Road, Cambridge CB2 1EZ, UK (email: deposit@ccdc.cam.ac.uk).

Additionally, IR spectra were recorded in KBr pellets for the studied compound. The data are presented in the Supplementary Information, but it has not been included in the main body of the text, because it does not deviate from the spectra published by Faniran and Shurvell in 1968.[32]

Computational methodology

Geometry optimization of the studied molecular complex was performed using DFT[27,28] and MP2 perturbation theory.[29] In the case of the DFT method, the hybrid functional of Becke coupled with the Lee, Yang and Parr correlation part, denoted henceforth as B3LYP[44,45] was applied during the study. Two different Gaussian basis-set schemes were used during the DFT and MP2 calculations: double- and triple-zeta split valence basis sets, augmented with polarization functions on all atoms and optionally diffuse functions on non-hydrogen atoms denoted according to Pople's nomenclature as 6-31G(d,p), 6-31+G(d,p), 6-311G(d,p) and 6-311+G(d,p), respectively.[46,47] Additionally, the harmonic frequency calculations were performed confirming that the final structures were local minima on the PES. The basis-set superposition error (BSSE) correction was calculated according to the Boys–Bernardi Scheme[48] during the DFT

Copyright © 2008 John Wiley & Sons, Ltd.

geometry minimization of the complex. The binding energy at the MP2 level was estimated at a separate step after the geometry optimization, therefore the DFT dimer structure includes BSSE corrections to the geometry[49] while the MP2 optimizations were not performed on a BSSE-corrected PES. This part of the calculations was performed using the Gaussian03 suite of programs,[50] which was also used to generate wavefunctions for subsequent topological analyses. In the next step, the AIM theory[30,51] was applied to study the topology of the electron density and intermolecular hydrogen bond properties on the basis of the density obtained from the DFT at the B3LYP/6-311+G(d,p) level of theory. The AIM analysis was carried out using the AIMPAC package.[52] ELF was calculated with TopMod suite.[53] Subsequently, the anharmonicity of the phenylboronic acid dimeric form was estimated by solving the 1D Schrödinger equation[34] for the simultaneous double proton motion in the intermolecular hydrogen bond. This allows for incorporation of the quantum nature of the proton motion by direct sampling of the *ab initio* PES. Due to the almost linear arrangement of the donor, proton and acceptor atoms in the optimized structure, the coordinates of the movable protons were obtained by simple interpolation between the oxygen sites retaining the centrosymmetric nature of the cyclic dimer (as in Fig. 1SI of the Supplementary Information). After excluding configurations with O. . .H distances smaller than 0.7 Å, 19 proton positions have been used for the PES sampling. The energy values were then used as the PES for the 1D vibrational quantum oscillator problem.[34] As the next step of the computational investigations, vibrational PED analysis was carried out using the Hessian obtained within the harmonic approximation at the B3LYP/6-31G(d,p) level. Consistently with the DFT optimization procedure described above, counterpoise BSSE corrections were also included during the harmonic frequency calculations. The GAR2PED program[54] was used for the PED analysis. Finally, the SAPT was applied to study the intermolecular interaction energy and decompose its value into physically significant contributions.[35] The SAPT2006 suite of programs[55] was used for this purpose, and necessary molecular integrals were obtained from the Gamess package[56] using the 6-311+G(d,p) basis set and the structures previously optimized at the B3LYP/6-311+G(d,p) level of theory. The BSSE corrections were also included in the geometry search preceding the SAPT analysis. As a last step of the computational part of the study, the CPMD[36] *in vacuo* was performed. The orthorhombic cell dimensions for the phenylboronic acid dimer were set to $a = 22.5$ Å, $b = c = 12$ Å. The size of the cell was dictated by the need to avoid artifacts at the cell boundary in isolated system calculation, for which the Hockney periodic image removal scheme was applied. The functional proposed by Handy and Cohen (OLYP)[57] in conjunction with the plane-wave basis set (cutoff = 70 Ry) was used for the study. The pseudopotentials of Troullier and Martins[58] types were used to replace the core electrons of the atoms. The initial period of the molecular dynamics (MD) (*ca.* 10 000 steps) was used to equilibrate the dimer and was omitted from the further discussion. The production MD data were collected for 13 ps. During the MD simulations, the time step was consistently set to 4 a.u. and a fictitious electron mass parameter (EMASS) of 400 a.u. was used to reproduce the orbital dynamics. The simulations were performed at $T = 100$ K and thermostated by Nosé–Hoover method.[59,60] The dipole moment values were collected during the MD run and subsequently used to generate the predicted IR spectrum of the studied compound. The contributions of lateral and bridged protons were calculated from the atomic velocities. The MD simulation on the DFT PES was performed using CPMD 3.11.1 program.[61] The graphical representation of the studied systems was prepared using the Diamond crystal and molecular visualization package[62] and VMD program.[63]

RESULTS AND DISCUSSION

The system under consideration is characterized by the presence of intermolecular hydrogen bonds, which are decisive for both molecular conformation and crystal packing. Available literature data contain structural description of the phenylboronic acid crystal at the room temperature.[25] The main aim of our redetermination of the structure under different conditions was to check the possibility of temperature-induced phase transitions or atom localization changes. According to our low-temperature study, an asymmetric unit comprises two molecules of the acid, which form a dimer (as in Fig. 1). The molecules essentially differ from each other by the twist of the —$B(OH)_2$ group with respect to the ring moiety. The angles between the best planes calculated for the C_{ring}—$B(OH)_2$ and the phenyl ring are 6.3° and 21.0° for the two independent molecules of the unit cell. This difference clearly indicates that the boronic group is highly flexible. Indeed, this twist angle in phenylboronic acids derivatives may differ from *ca.* 0° in 4-bromophenylboronic acid[23,64] upto *ca.* 35° in 3-bromophenylboronic acid,[65] while the mean value and the standard deviation of this angle are *ca.* 11° and 9°, respectively.[26] The details of the crystal packing are provided in Fig. 2. The dimeric ensemble (consisted of molecules A and B) is related by the twofold axis along [001] direction with another dimeric unit. Both these units are linked by hydrogen bonds with another

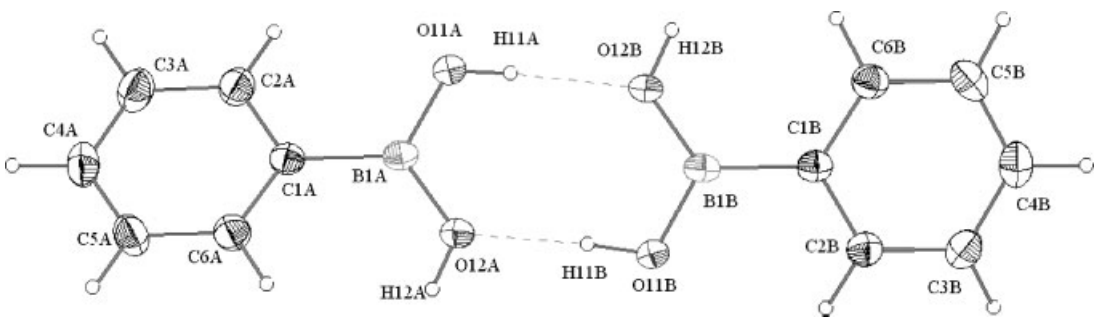

Figure 1. Molecular structure of the studied phenylboronic acid dimer. The intermolecular hydrogen bonds are marked as dotted lines. The displacement parameters are drawn at 50% probability level

Copyright © 2008 John Wiley & Sons, Ltd.

Journal of Physical Organic Chemistry

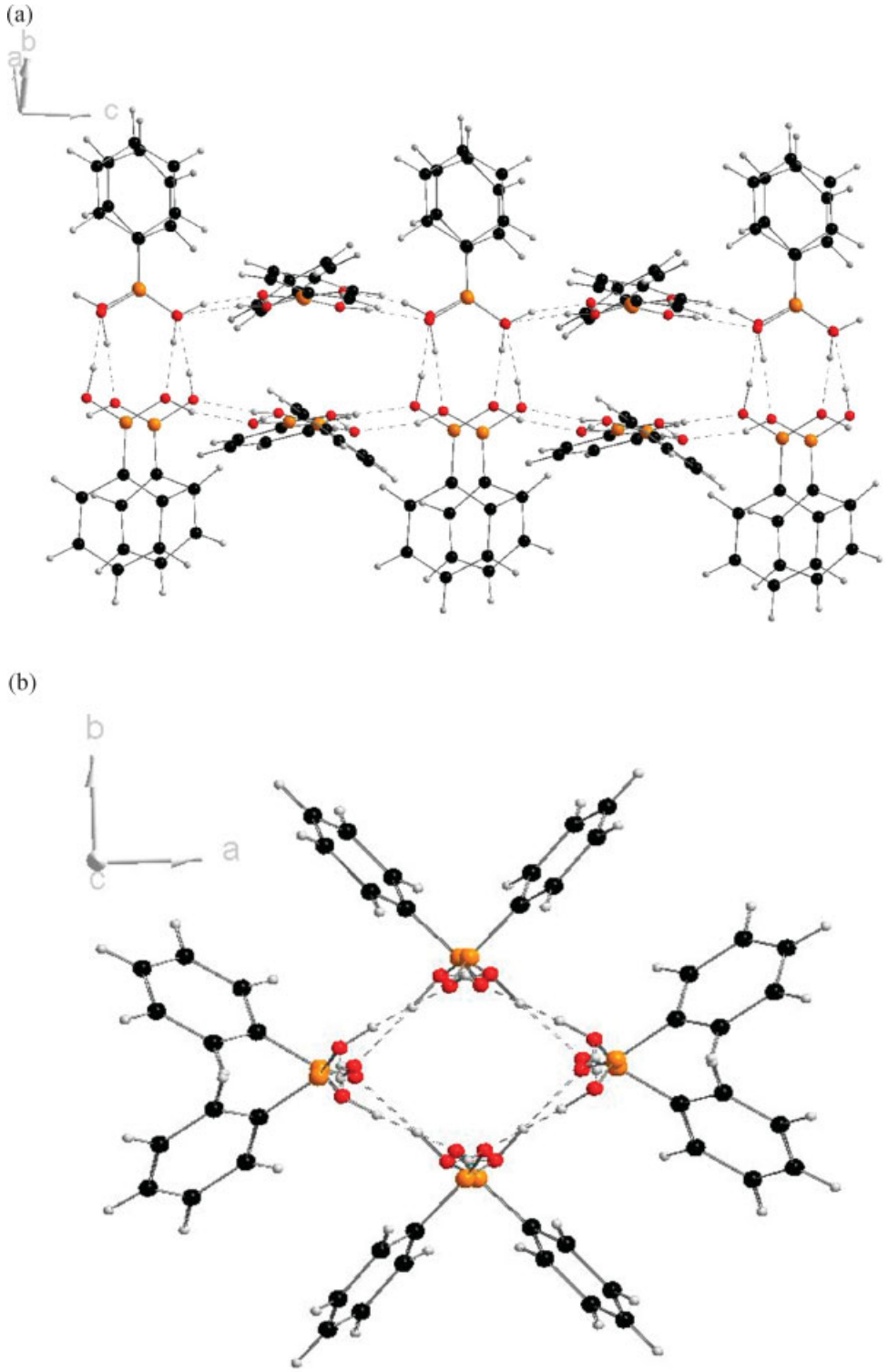

Figure 2. The intermolecular interactions in the crystal lattice of phenylboronic acid. (a) View along [110] direction. (b) View along [001] direction

pair of dimers which are turned by *ca.* 76.7° (the mean angle between best planes for the dimers), as shown in Fig. 2(a) (view along [110] direction). These units are generated by reflection of given pair of dimers in c-glide planes lying parallel to the twofold axis. An infinite channel built of the symmetry-related dimers having cc2 symmetry is formed in this way (as in Fig. 2(b)).

Although the dimer is the most basic structural motif in the crystal lattice of phenylboronic acid, from the geometrical point of view the hydrogen bonds formed between the dimeric ensembles are somewhat stronger compared with the hydrogen bonds forming the dimers: the H···O distances are 1.885 Å (O···O distances are 2.692 and 2.709 Å) for the former case and 1.888 and 1.805 Å (O···O distances are 2.734 and 2.721 Å) for the

 Copyright © 2008 John Wiley & Sons, Ltd.

Table 1. Selected experimental and calculated geometrical parameters for the phenylboronic acid dimer. The results are presented only for the basis sets with diffuse functions

		DFT, B3LYP		MP2	
Geom. parameters	Exp. mol. A/B[a]	6-31+G(d,p)	6-311+G(d,p)	6-31+G(d,p)	6-311+G(d,p)
Bond lengths (Å)					
O–H (bridge)	0.85(2)/0.92(2)	0.977	0.974	0.977	0.973
O···O	2.721(2)/2.734(2)	2.858	2.854	2.827	2.821
H···O	1.81(2)/1.89(3)	1.882	1.879	1.852	1.848
O–H (free)	0.85(2)/0.88(3)	0.964	0.960	0.965	0.962
B–O (acceptor)	1.366(2)/1.365(2)	1.394	1.392	1.340	1.400
B–O (donor)	1.369(2)/1.369(2)	1.355	1.353	1.359	1.354
B–C	1.556(2)/1.562(3)	1.570	1.567	1.567	1.569
Valence angles (°)					
O–H···O	175(3)/175(3)	179.23	179.28	176.18	178.74
O–B–O	115.9(2)/116.0(2)	117.85	117.82	118.48	118.75

[a] The asymmetric unit of the crystal cell contains two nonequivalent molecules A and B, but the small difference between them – the arrangement of the acidic group – is a result of crystal packing forces. The differences in bond length are smaller than 3 σ. It is therefore irrelevant for gas-phase DFT and MP2 calculations, and the distinction between A and B is thus dropped in the computational part.

latter. Similarly as in the case of the room-temperature structure,[25] the CBO_2 units are planar (within the experimental error) and the boronic group has a trigonal geometry. Overall, the crystal and molecular structure of the phenylboronic acid at 100 K is fairly similar to that observed at 295 K.[25] Selected bond lengths, bond angles, and torsion angles are given in Tables 1SI, 2SI, and 3SI of the Supplementary Information, respectively.

As the second part of our structural study of the phenylboronic acid, an extensive computational description was carried out. The selected geometrical parameters (experimental and calculated) pertaining to the boron atom and the intermolecular hydrogen bond are presented in Table 1. The bond lengths and valence angle values are presented only for basis sets with diffuse functions for both levels of theory applied during the calculations. The basic structural descriptor of the hydrogen bond, O···O distance in the equilibrium structure of the dimer, has been correctly reproduced by the applied DFT and MP2 methods with respect to the experiment. The difference between calculated and experimental value of the O···O distance is *ca.* 0.13 Å for the DFT and 0.10 Å for MP2 method, respectively. The elongation of the calculated hydrogen bond lengths should be attributed to the lack of crystal packing forces and electrostatic interactions with neighboring molecules in the theoretical model (isolated dimer, as in Fig. 1SI). It is worth to mention that the presented calculated geometrical parameters are in a very good agreement with the previous report on the gas phase and solid-state investigations of a family of carboxylic and boronic acid dimers[19] (the O···O distance of 2.826 Å in Reference [19] and 2.827 Å in the present study at the comparable level of theory). The values of O—H and H···O distances (Table 1) revealed no significant shift of hydrogen-bonded protons toward the acceptor, and suggest that the intermolecular interactions could be classified as medium-strong hydrogen bonds. However, B—O (acceptor) distance is generally elongated compared to the experimental data, whereas the B—O (donor) distance was reproduced quite well. The disagreement could be due to the degrees of freedom in gas phase and the absence of the neighboring molecules as well to the fact that the O acceptor is able to form hydrogen bonds with the lateral neighbors in the crystal. The values of dimerization energies (Tables 2 and 3) are in agreement with this observation. The O—H···O valence angle values (as in Table 1) show that the MP2 method gave results closer to the experimental findings than the DFT method. The O—B—O angle corresponds to the sp^2 hybridization on the boron atom. The similarity of the calculated DFT and MP2 geometrical parameters suggests that the dispersion forces do not play a crucial role in the dimer formation. This fact is also supported by the binding energies presented in Tables 2 and 3, respectively, for the DFT and MP2 methods. Literature study showed that for carboxylic acid dimers[66] the situation is highly similar and the performance of the B3LYP functional was very satisfactory in comparison with the reference G2(MP2) method. However, it is worth mentioning that the dimerization energies of carboxylic acids are over twice as high as those of the studied phenylboronic acid. The BSSE was also estimated for both applied methods in the study (as in the 'Computational Methodology' section and Tables 2 and 3). The interaction

Table 2. Binding energy for the studied dimer of the phenylboronic acid calculated with B3LYP DFT functional (including vibrational zero point correction and basis-set superposition error (BSSE)). The value of BSSE is also given

Level of theory	Binding energy (kcal/mol)	BSSE (kcal/mol)
6-31G(d,p)	−8.052	2.770
6-31+G(d,p)	−7.616	0.967
6-311G(d,p)	−7.671	2.535
6-311+G(d,p)	−7.555	0.750

Copyright © 2008 John Wiley & Sons, Ltd.

Journal of Physical Organic Chemistry

Table 3. Binding energy for the studied dimer of the phenylboronic acid calculated at the MP2 level (including *a posteriori* basis-set superposition error (BSSE))

Level of theory	Binding energy (kcal/mol)	BSSE (kcal/mol)
6-31G(d,p)	−8.082	3.725
6-31+G(d,p)	−7.318	3.650
6-311G(d,p)	−7.171	3.958
6-311+G(d,p)	−6.863	3.152

energies reported here are in very good agreement with those computed previously[19] for the phenylboronic acid dimer, if the BSSE correction is not included (−12.9 kcal/mol in Reference [19], −11.8 kcal/mol in the present study at MP2/6-31G(d,p) level of theory). The obtained values in the case of the DFT method showed that the addition of the diffuse functions reduces the BSSE significantly. The BSSE reduction is much smaller for MP2 (Table 3). Larger values of the BSSE correction for explicitly correlated methods (such as MP2) with respect to DFT are frequently encountered. The increase in the BSSE is a result of the fact that post-Hartree–Fock electron correlation techniques explore the subspace of virtual orbitals, while DFT includes correlation effects by means of the E_{xc} functional using only occupied orbitals. As the further part of the computational study, the analysis of the electron-density topology was performed according to the AIM theory. The electron density cross-section obtained at the DFT B3LYP/6-311+G(d,p) level of theory is presented in Fig. 3. The AIM theory was applied to observe the manifestation of a pair of intermolecular hydrogen bonds in the studied dimer. According to the AIM framework, between linked atoms there are unique points with maximum electron density along the interatomic path, which are related to the presence of bonds between these atoms. The points are called bond critical points (BCPs) and give insight into the network of bonds in studied molecules. In the case of phenylboronic acid, the presence of two BCPs between monomers and corresponding bond paths is a result of the formation of a pair of intermolecular

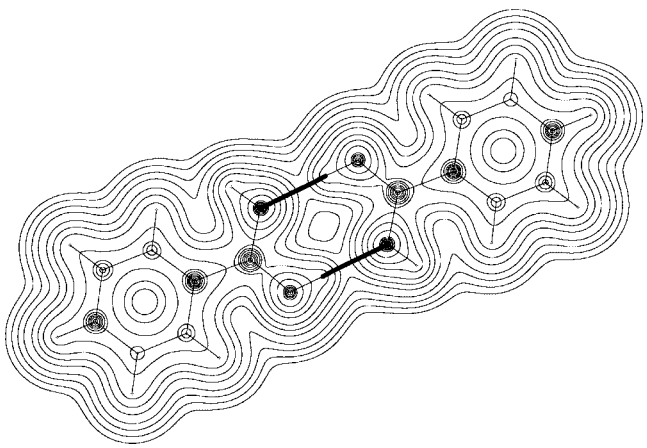

Figure 3. Electron density cross-section in the plane defined by the atoms in the pair of hydrogen bonds. The bond paths of the intermolecular hydrogen bonds are marked by thick lines. Results obtained from the DFT at the B3LYP/6-311+G(d,p) level of theory

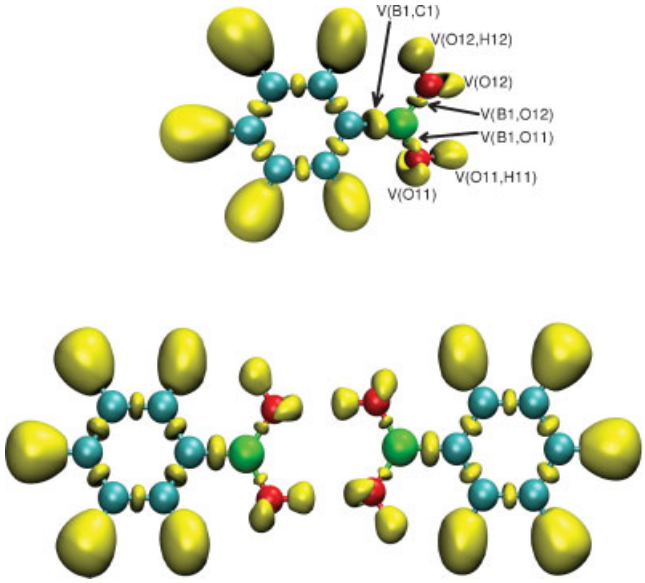

Figure 4. Electron localization function (ELF) isosurface (ELF = 0.86) for the monomeric (top) and dimeric (bottom) forms of the studied phenylboronic acid

hydrogen bonds. Visible differences in the density of isolines for aromatic carbon atoms are results of the fact that Fig. 3 presents a cross-section through a computational model of the dimer in the plane defined by the pair of hydrogen bonds. The phenyl rings are therefore slightly displaced from the drawing plane. The extension of our topological analysis of the electronic structure by the ELF analysis is presented in Fig. 4 and Table 4. The partitioning of the molecular space into localization basins according to the ELF analysis locates atomic core regions and electron pair domains. Figure 4 describes such a partitioning for the phenylboronic acid monomer and dimer. The comparison of the two forms shows that the formation of the pair of hydrogen bonds does not change the topological features of the ELF scalar field. Additional observation of the decomposition of the 3D space into domains of different ELF value indicated that the dimer cannot be classified as 'strongly bound' in the sense of topological definition of hydrogen bond strength.[67,68] More details of the bonding are revealed in the spatial volume and electronic population of the basins corresponding to the core electrons, covalent bonds, and lone pairs of the investigated systems (Table 4). The core electrons, in agreement with their chemical inertness, are not affected by the formation of the dimer. The B1—C1 bond is also only slightly perturbed. The most important changes involve strengthening of the B1—O11 bond (electron population rises from 2.07 e to 2.19 e), simultaneous small inflow of the electron density to the H11 atom (from 1.75 e to 1.79 e), and large decrease in the population of the O11 lone pairs (from 4.01 e to 3.86 e). This corresponds to the physical process of the electron transfer from the lone pairs of the donor toward the hydrogen atom involved in the intermolecular hydrogen bond. The H12 hydrogen atom is almost not affected by the formation of the dimeric form. Systems containing intermolecular hydrogen bonds are potentially highly anharmonic. The anharmonicity is an important property from the spectroscopic point of view, and it can be responsible for many application-related processes at the molecular level. As a step

 Copyright © 2008 John Wiley & Sons, Ltd.

Table 4. Population of ELF mono- and disynaptic basins corresponding to the core electrons, bonding, and free electron pairs

	Monomer		Dimer	
Basin definition	Volume [a_0^3]	Population [e]	Volume [a_0^3]	Population [e]
C(B1)	1.67	2.07	1.69	2.07
C(C1)	0.81	2.09	0.80	2.09
C(O11)	0.26	2.11	0.26	2.12
C(O12)	0.26	2.11	0.26	2.11
V(B1, C1)	66.83	2.51	65.46	2.50
V(B1, O11)	18.99	2.07	22.08	2.19
V(B1, O12)	19.05	2.03	18.23	2.00
V(O11, H11)	49.11	1.75	27.73	1.79
V(O12, H12)	43.25	1.76	42.20	1.75
V(O11)	100.07	4.01	98.24	3.86
V(O12)	107.62	4.04	85.37	4.07

forward of our analysis, we have constructed the DFT PES for the simultaneous proton motion in the bridge, with a subsequent solution of the 1D vibrational Schrödinger equation and calculation of anharmonic energy levels with corresponding wavefunctions. The results are shown in Fig. 5. The calculated wavenumber for the $0 \rightarrow 1$ vibrational transition is 3368.6 cm^{-1}, and the corresponding harmonic value for the symmetric O—H stretching mode is 3609 cm^{-1} (refer detailed description of the PED analysis below, and Table 5). The experimental position of the center of the broad O—H absorption in the KBr spectrum of the phenylboronic acid[32] is located at 3280 cm^{-1}, while our IR measurements indicate that the maximal absorption in the high-wavenumber range is located at 3428 cm^{-1} (as in Fig. 2SI of the Supplementary Information). The difference between our anharmonic result and the experimental band position can be attributed to the strong polar field of the molecular crystal. The PES exhibits a shoulder at the position of the proton close to the acceptor site, but the energy of the plateau is rather high – *ca.* 40 kcal/mol related to the equilibrium position. As a natural next step of the vibrational study, we have performed the PED analysis for the harmonic normal modes. The harmonic vibrational frequencies of the phenylboronic acid dimer calculated with the DFT B3LYP functional and various Pople double- and triple-zeta split valence basis sets are converged to within 10–20 cm^{-1}. Table 5 lists the most relevant vibrational modes of the neighborhood of the boron atom with their calculated PED assignment (a complete PED analysis is to be found in the Supplementary Information, Table 4SI). The structure of the dimer suggests that the boronic acids, contrary to the carboxylic analogues, will exhibit simultaneously both free and hydrogen-bonded O—H stretching modes. This will not be necessarily true in the condensed phase, where free OH bonds might be used to form intermolecular hydrogen bonds linking separate dimeric units. This is, in fact, true for the analyzed crystal of the

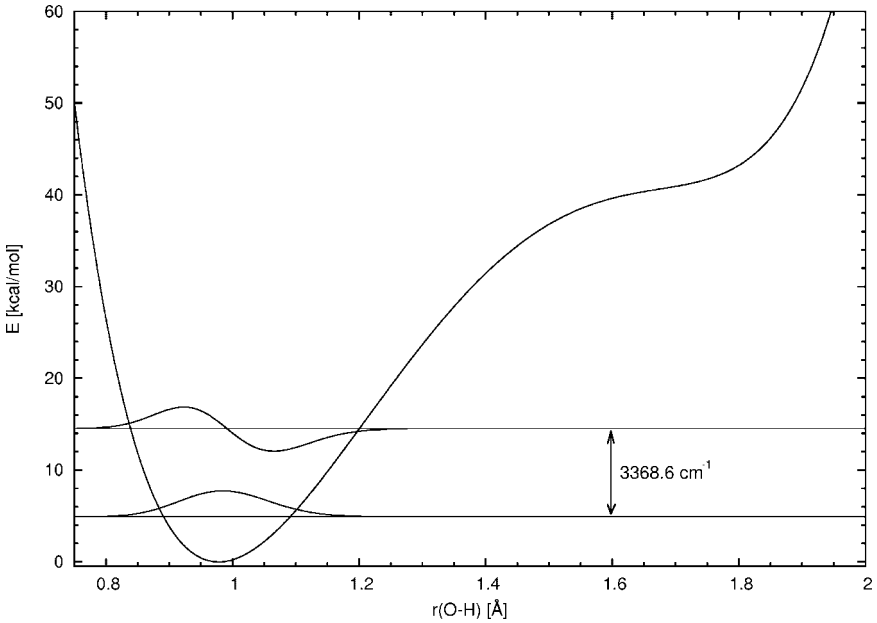

Figure 5. Potential energy surface and anharmonic vibrational energy levels for the proton movement in the hydrogen bond of the phenylboronic acid dimer

Copyright © 2008 John Wiley & Sons, Ltd.

Table 5. Potential energy distribution of the phenylboronic acid dimer, calculated at the B3LYP/6-31G(d,p) BSSE-free level within the harmonic approximation. Data for OH groups and surroundings of the boron atom are presented

Mode	ν (cm^{-1})	Intensity (km/mol)	Assignment	Internal coordinates
49	1050	150	$\nu^{\text{br.O-H}}_{\text{bend.}}$	$\nu^{\text{B1'-O11'-H11'}}_{\text{bend}}(24\%) - \nu^{\text{B1-O12-H12}}_{\text{bend}}(22\%) + \nu^{\text{B1-O12'-H12'}}_{\text{bend}}(22\%)$
51	1080	261	$\nu^{\text{br.O-H}}_{\text{bend.}}$	$\nu^{\text{B1'-O11'-H11'}}_{\text{bend}}(25\%) + \nu^{\text{B1-O12-H12}}_{\text{bend}}(24\%) - \nu^{\text{B1-O12'-H12'}}_{\text{bend}}(24\%)$
55	1180	137	$\nu^{\text{br.O-H}}_{\text{bend.}}$	$\nu^{\text{B1'-O11'-H11'}}_{\text{bend}}(26\%) - \nu^{\text{B1-O12-H12}}_{\text{bend}}(23\%) + \nu^{\text{B1-O12'-H12'}}_{\text{bend}}(23\%)$
66	1378	939	$\nu^{\text{br.O-H}}_{\text{bend.}}$	$\nu^{\text{B1'-O11'-H11'}}_{\text{bend}}(31\%)$
68	1455	337	$\nu^{\text{B-O}}_{\text{asym.str.}}$	$\nu^{\text{B1-O11}}_{\text{str}}(24\%) - \nu^{\text{B1'-O11'}}_{\text{str}}(24\%)$
70	1490	275	$\nu^{\text{B-O}}_{\text{asym.str.}}$	$\nu^{\text{B1-O11}}_{\text{str}}(14\%) - \nu^{\text{B1'-O11'}}_{\text{str}}(14\%) - \nu^{\text{C1-B1-O11}}_{\text{bend}}(13\%) - \nu^{\text{C1'-B1'-O11'}}_{\text{bend}}(8\%)$
87	3609	0	$\nu^{\text{br.OH}}_{\text{sym.str.}}$	$\nu^{\text{O11-H11}}_{\text{str}}(34\%) + \nu^{\text{O11'-H11'}}_{\text{str}}(34\%) - \nu^{\text{O12'...H11}}_{\text{str}}(16\%) - \nu^{\text{O12...H11'}}_{\text{str}}(16\%)$
88	3638	2338	$\nu^{\text{br.OH}}_{\text{asym.str.}}$	$\nu^{\text{O11-H11}}_{\text{str}}(34\%) - \nu^{\text{O11'-H11'}}_{\text{str}}(34\%) - \nu^{\text{O12'...H11}}_{\text{str}}(16\%) + \nu^{\text{O12...H11'}}_{\text{str}}(16\%)$
89	3872	60	$\nu^{\text{freeOH}}_{\text{asym.str.}}$	$\nu^{\text{O12-H12}}_{\text{str}}(48\%) - \nu^{\text{O12'-H12'}}_{\text{str}}(51\%)$
90	3872	2	$\nu^{\text{freeOH}}_{\text{sym.str.}}$	$\nu^{\text{O12-H12}}_{\text{str}}(51\%) + \nu^{\text{O12'-H12'}}_{\text{str}}(48\%)$

phenylboronic acid, as described above. Therefore, no free O—H stretching mode frequencies were located experimentally. However, gas-phase dimer calculations allow us to probe a possible mixing of the free and hydrogen-bonded O—H stretching modes. As shown in Table 5, this does not happen and the two highest levels are indeed pure free O—H stretching modes. These symmetric and antisymmetric modes are almost degenerate, indicating the lack of coupling between the free O—H groups. On the other hand, the two low-lying modes (87 and 88), which are responsible for the hydrogen bond stretching, exhibit a 230–260 cm^{-1} red shift with respect to the free O—H stretching. Typically, for the hydrogen bond, the intensity of the $\nu_{\text{asym.str.}}$ mode is increased almost 40 times when compared to the free OH $\nu_{\text{asym.str.}}$ Remaining modes of significant intensity are also connected with the hydrogen bond or the boron atom. The antisymmetric doublet at 1455 and 1490 cm^{-1} is related to the B—O stretching modes, while B—O—H and hydrogen bond bending modes are visible at 1050, 1080, 1180 and, notably, 1378 cm^{-1}. The last two modes contain also a small admixture of the B—O stretching, which is not otherwise visible in the PED analysis. In the next part of our computational study, we have analyzed the interaction energy for a set of systems analogous to the phenylboronic acid dimer (as in Fig. 6). We have not found detailed description of interaction energy terms for boronic acids dimers in the literature. The comparison of such systems with the classical case of carboxylic acids was also particularly interesting for us. According to the SAPT formulation, the interaction energy was partitioned into the following contributions:

$$E^{\text{SAPT}} = E^{10}_{\text{elst}} + E^{10}_{\text{exch}} + E^{10}_{\text{ind,r}} + E^{20}_{\text{exch-ind,r}} + \delta HF_{\text{int,r}} + E^{12}_{\text{elst,r}} + E^{13}_{\text{elst,r}} + E^{20}_{\text{disp}} + E^{20}_{\text{exch-disp}} + {}^{t}E^{22}_{\text{ind}} + {}^{t}E^{22}_{\text{exch-ind}} + \varepsilon^{1}_{\text{exch}}(\text{CCSD}) + \varepsilon^{2}_{\text{disp}}(2)$$

The most important of these contributions are listed in Table 6, while detailed results are given in Table 5SI of the Supplementary Information. The basic contributions to the interaction energy are: E^{10}_{elst} (electrostatic interaction of the frozen charge distributions of the monomers), E^{10}_{exch} (repulsion force due to the quantum exchange phenomenon), $E^{20}_{\text{ind,r}}$ (result of the mutual

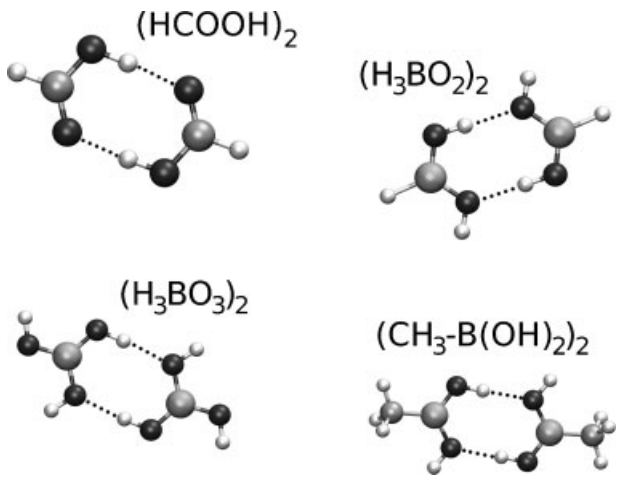

Figure 6. Structures of hydrogen-bonded dimers used in the SAPT interaction energy analysis. From top to bottom: formic acid dimer, H–B(OH)$_2$ dimer, HO–B(OH)$_2$ dimer, CH$_3$–B(OH)$_2$ dimer. Color coding of atoms: blue, carbon; green, boron; red, oxygen; white, hydrogen

Copyright © 2008 John Wiley & Sons, Ltd.

Table 6. Selected terms of the SAPT interaction energy partitioning for the phenylboronic acid dimer analogues

SAPT results	(H_2O) dimer[69]	(HCOOH) dimer	$(H–B(OH)_2)$ dimer	$(HO–B(OH)_2)$ dimer	$(CH_3–B(OH)_2)$ dimer
E^{10}_{elst}	−7.79	−31.22	−18.18	−20.05	−18.56
E^{10}_{exch}	6.16	30.83	16.24	17.52	16.59
$E^{20}_{ind,r}$	−2.13	−17.83	−7.46	−8.09	−7.51
$E^{20}_{exch-ind,r}$	N/A	9.31	4.06	4.19	4.11
SCF SAPT	**−3.76**	**−8.91**	**−5.34**	**−6.42**	**−5.37**
δHF	N/A	−6.26	−2.45	−2.67	−2.47
$E^{2}_{disp,k}$	−2.49	−8.50	−5.52	−5.79	−5.79
$E^{20}_{exch-disp}$	0.36	1.58	0.88	0.91	0.92
$SAPT_{corr,r}$	−1.88	−0.13	−1.34	−1.47	−1.54
$SAPT_r$	**−5.45**	**−15.30**	**−9.13**	**−10.56**	**−9.37**

Additional data for water dimer from Reference [69] do not include response corrections.

polarization of the charge distributions of the monomers), $E^{20}_{exch-ind,r}$ (correction to the exchange resulting from the polarization). These terms do not include intra-monomeric electron correlation. Together with a correction term *δHF*, they correspond to the Hartree–Fock interaction energy. Among the correlation corrections, we report the most important ones: E^{20}_{disp} (dispersion energy) and $E^{20}_{exch-disp}$ (contributions to the exchange repulsion resulting from dispersion effects). As shown by our analysis, carboxylic acid dimers (here represented by formic acid) have significantly larger interaction energy, thus forming stronger hydrogen bonds. The difference in the energies is visible already at the uncorrelated level (SAPT SCF, as in Table 6). In all cases, the electrostatic term E^{10}_{elst} is almost compensated by the exchange repulsion E^{10}_{exch}, but the compensation is less pronounced in case of the boronic acids. This means that electron densities of the monomers have larger overlap for carboxylic acids, leading to increased exchange repulsion. However, this effect is overruled by a visibly smaller induction contribution for the boronic acid dimers. Additionally, the correction term *δHF* gathering higher order terms is also much larger for the formic acid dimer, which might signify that the carboxylic pair of hydrogen bonds is more covalent than in the boronic acids. The correlation corrections are larger for the boronic acids than for the formic acid, but they do not form a significant part of the interaction energy ($SAPT_{corr,r}$ in Table 6). Thus, we attribute weaker hydrogen bonds in the boronic acid dimers with respect to the carboxylic analog to the smaller polarization effects. A general comparison with prototypic hydrogen-bonded system, water dimer,[69] is also included in Table 6. Hydrogen bonds, as opposed to weaker van der Waals interactions, exhibit rather large electrostatic and exchange energy contributions. Neither polarization nor dispersion terms are dominating the energy. This is true for all of the studied systems, as well as for the water dimer. Taking into consideration that $(H_2O)_2$ has a single hydrogen bond, while the dimers studied here have a pair of such bonds, the results presented in Table 6 indicate similarity between various types of O—H. . .O contacts. In the final step, the results obtained by the CPMD are discussed. The constructed gas-phase dynamical model allows us to observe the presence or absence of molecular events related, for example, to the hydrogen bond as functions of time. Such events are not visible directly in the static gas-phase models or time-unresolved experiments (e.g. X-ray or IR measurements). Our special attention was paid to the intermolecular hydrogen bonds in the studied dimer. The average values of the metric parameters of the intermolecular hydrogen bond are: donor. . .acceptor distance is 3.214 Å while the donor–hydrogen is 0.974 Å and hydrogen. . .acceptor 2.259 Å. The obtained average values suggest that although the hydrogen bond is not strong, the dimer is stable. The graphical representation of the vibrational properties is presented in Fig. 7. Special attention was paid to the spectroscopic features of the lateral and bridge protons. Figure 7 shows that the absorption ranging from 3380 to 3620 cm^{-1} corresponds to the O—H stretching. However, the lateral, not hydrogen-bonded protons, oscillate at a very sharply defined wavenumber of 3620 cm^{-1}. The bridged protons are red-shifted and occupy the range from 3380 to 3600 cm^{-1} centered at 3500 cm^{-1}. The red shift of 120 cm^{-1} between positions of bridged and lateral protons is a measure of the strength of interactions in the hydrogen bond. It is worth to mention that the features of the lower frequencies region are rather similar and we could not localize the frequencies associated with the particular proton types on the basis of the dipole spectrum. Therefore, the vibrational study was enhanced by the use of the atomic velocities spectra of the lateral and bridged protons.

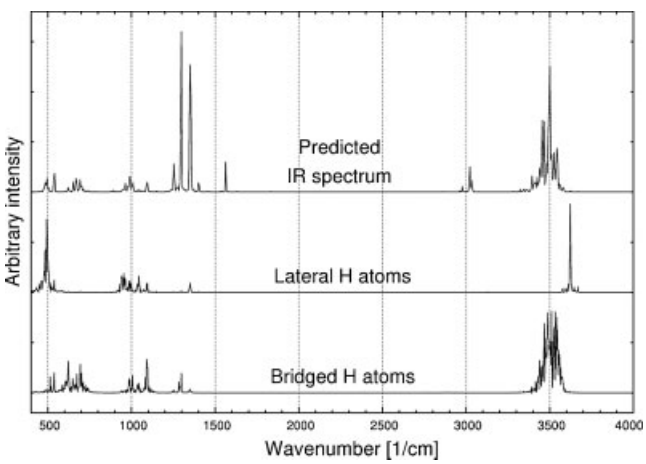

Figure 7. Predicted infrared spectrum of the studied phenylboronic acid dimer (upper) and contributions of lateral and bridged hydrogen atoms as a result of *ab initio* molecular dynamics *in vacuo*

Copyright © 2008 John Wiley & Sons, Ltd.

The current study presents a detailed computational description of a member of boronic acid family supported by low-temperature X-ray measurements. The use of a large variety of methods provides quantitative and qualitative information useful from the point of view of spectroscopy, structural chemistry, and material science. CPMD was found to be a useful method of description and understanding of the chemical properties of the boronic acids at the molecular level significant for the future applications of these compounds in various branches of chemistry.

CONCLUSIONS

The properties of phenylboronic acid were studied by the application of experimental and theoretical methods. The cyclic dimer was found as the basic building block of the molecular crystal, similar to the experiments performed at room temperature.[25] Subsequently, the extensive network of hydrogen bonds linking dimers in the crystal was described. An isolated dimer of the phenylboronic acid was a target for the computational study. The bridge protons were found to be located at the donor sites indicating that the proton transfer phenomena do not occur in the studied dimeric form of the phenylboronic acid. Topological analysis of the molecular scalar fields was used to discuss the bonding pattern in the system confirming the presence of the pair of intermolecular hydrogen bonds, which could be classified as medium-strong. Harmonic PED analysis suggests that, despite small frequency difference, the vibrations of the free and hydrogen-bonded OH groups do not mix. SAPT study revealed that decrease in polarization term is responsible for lower interaction energies with respect to formic acid dimer.

SUPPLEMENTARY MATERIAL

Detailed description of the crystal structure and information for full retrieval of the crystal data, visualization of the studied dimer, IR experimental spectra, extended output of programs for PED, and SAPT analyses are provided in the supplementary material.

Acknowledgements

A. J. and J. J. P. would like to thank to Dr Jamieson K. Christie for a fruitful discussion and useful comments during the preparation of the paper. A. J. and J. J. P. gratefully acknowledge the Wrocław Center for Networking and Supercomputing (WCSS), the Academic Computer Center CYFRONET-KRAKÓW (Grants KBN/SGI/UWrocl/029/1998 and KBN/SGI/UWrocl/078/2001), and the Poznań Supercomputing and Networking Center for providing computer time and facilities. P. K., M. K. C., and A. S. gratefully acknowledge the financial support from the Ministry of Science and Higher Education (Grant N204 01932/0614).

REFERENCES

[1] Ed.: D. G. Hall, *Boronic Acids. Preparation, Applications in Organic Synthesis and Medicine*, Wiley-VCH, Weinheim, **2005**.
[2] K. E. Maly, N. Malek, J.-H. Fournier, P. Rodriguez-Cuamatzi, T. Maris, J. D. Wuest, *Pure Appl. Chem.* **2006**, *78*, 1305.
[3] N. Miyaura, A. Suzuki, *Chem. Rev.* **1995**, *95*, 2457.
[4] N. A. Petasis, I. Akritopoulou, *Tetrahedron Lett.* **1993**, *34*, 583.
[5] A. H. Soloway, W. Tjarks, R. A. Barnum, F. G. Rong, R. F. Barth, I. M. Codogni, J. G. Wilson, *Chem. Rev.* **1998**, *98*, 1515.
[6] S. K. Kumar, E. Hager, C. Pettit, H. Gurulingappa, N. E. Davidson, S. R. Khan, *J. Med. Chem.* **2003**, *46*, 2813.
[7] J. D. Dunitz, D. M. Hawley, D. Miklos, D. N. White, Y. Berlin, R. Marusic, V. Prelog, *Helv. Chim. Acta* **1971**, *54*, 1709.
[8] H. Nakumura, Y. Iitacaka, T. Kitahara, T. Okasaki, Y. Okami, *J. Antibiot.* **1977**, *30*, 714.
[9] A. M. Irving, C. M. Vogels, L. G. Nikolcheva, J. P. Edwards, X. F. He, M. G. Hamilton, M. O. Baerlocher, A. Decken, S. A. Wescott, *New. J. Chem.* **2003**, *27*, 1419.
[10] J. Myung, K. B. Kim, C. M. Crews, *Med. Res. Rev.* **2001**, *21*, 245.
[11] A. B. Shenvi, *Biochemistry* **1986**, *25*, 1286.
[12] R. Baggio, D. Elbaum, Z. F. Kanyo, P. J. Carroll, R. C. Cavalli, D. E. Ash, D. W. Christianson, *J. Am. Chem. Soc.* **1997**, *119*, 8107.
[13] W. Wang, X. Gao, B. Wang, *Curr. Org. Chem.* **2002**, *6*, 1285.
[14] T. D. James, S. Shinkai, *Top. Curr. Chem.* **2002**, *218*, 159.
[15] T. D. James, M. D. Phillips, S. Shinkai, *Boronic Acids in Saccharide Recognition*, RCS Publishing, Cambridge, **2006**.
[16] J.-H. Fournier, T. Maris, J. D. Uest, W. Guo, E. Galoppini, *J. Am. Chem. Soc.* **2003**, *125*, 1002.
[17] D. Braga, M. Polito, M. Bracaccini, D. D'Addario, E. Tagliavini, L. Sturba, *Organometallics* **2003**, *22*, 2142.
[18] V. R. Pedireddi, N. SeethaLekshmi, *Tetrahedron Lett.* **2004**, *45*, 1903.
[19] P. Rodriguez-Cuamatzi, O. I. Arillo-Flores, M. I. Bernal-Uruchurtu, H. Höpfl, *Cryst. Growth Des.* **2005**, *5*, 167.
[20] N. SeethaLekshmi, V. R. Pedireddi, *Cryst. Growth Des.* **2007**, *7*, 944.
[21] P. Rodriguez-Cuamatzi, G. Vargas-Diaz, H. Höpfl, *Angew. Chem. Int. Ed.* **2004**, *43*, 3041.
[22] P. Rogowska, M. K. Cyrański, A. Sporzyński, A. Ciesielski, *Tetrahedron Lett.* **2006**, *47*, 1389.
[23] M. R. Shimpi, N. SeethaLekshmi, V. R. Pedireddi, *Cryst. Growth Des.* **2007**, *7*, 1958.
[24] A. Sporzyński, *Pol. J. Chem.* **2007**, *81*, 757.
[25] S. J. Rettig, J. Trotter, *Can. J. Chem.* **1977**, *55*, 3071.
[26] F. H. Allen, J. E. Davies, J. J. Galloy, O. Johnson, O. Kennard, M. E. McRae, G. F. Mitchell, J. M. Smith, D. G. Watson, *J. Chem. Inf. Comput. Sci.* **1991**, *31*, 187.
[27] P. Hohenberg, W. Kohn, *Phys. Rev.* **1964**, *136*, B864.
[28] W. Kohn, L. J. Sham, *Phys. Rev.* **1965**, *140*, A1133.
[29] C. Møller, M. S. Plesset, *Phys. Rev.* **1934**, *46*, 618.
[30] R. F. W. Bader, *Atoms in Molecules, A. Quantum Theory*, Clarendon Press, Oxford, **1990**.
[31] B. Silvi, A. Savin, *Nature* **1994**, *371*, 683.
[32] J. A. Faniran, H. F. Shurvell, *Can. J. Chem.* **1968**, *46*, 2089.
[33] E. B. Wilson, J. C. Decius, P. C. Cross, *Molecular Vibrations: The Theory of Infrared and Raman Vibrational Spectra*, McGraw-Hill, New York, **1955**.
[34] J. Stare, J. Mavri, *Comput. Phys. Commun.* **2002**, *143*, 222.
[35] B. Jeziorski, R. Moszyński, K. Szalewicz, *Chem. Rev.* **1994**, *94*, 1887.
[36] R. Car, M. Parrinello, *Phys. Rev. Lett.* **1985**, *55*, 2471.
[37] S. Miura, M. E. Tuckerman, M. L. Klein, *J. Chem. Phys.* **1998**, *109*, 5290.
[38] P. R. L. Markwick, N. L. Doltsinis, D. Marx, *J. Chem. Phys.* **2005**, *122*, 054112.
[39] G. S. Hwang, W. A. Goddard, III, *Appl. Phys. Lett.* **2003**, *83*, 1047.
[40] A. Gambirasio, M. Bernasconi, *Phys. Rev. B* **1999**, *60*, 12007.
[41] G. M. Sheldrick, *Acta Cryst. A* **1990**, *46*, 467.
[42] G. M. Sheldrick, *SHELXL93. Program for the Refinement of Crystal Structures*, University of Göttingen, Germany.
[43] Ed.: A. J. C. Wilson, *International Tables for Crystallography, Vol. C*, Kluwer, Dordrecht, **1992**.
[44] A. D. Becke, *J. Chem. Phys.* **1993**, *98*, 5648.
[45] C. Lee, W. Yang, R. G. Parr, *Phys. Rev. B* **1988**, *37*, 785.
[46] R. Ditchfield, W. J. Hehre, J. A. Pople, *J. Chem. Phys.* **1971**, *54*, 724.
[47] R. Krishnan, J. S. Binkley, R. Seeger, J. A. Pople, *J. Chem. Phys.* **1980**, *72*, 650.
[48] S. F. Boys, F. Bernardi, *Mol. Phys.* **1970**, *19*, 553.
[49] S. Simon, M. Duran, J. J. Dannenberg, *J. Chem. Phys.* **1996**, *105*, 11024.
[50] Gaussian 03, Revision A.01, M. J. Frisch, G. W. Trucks, H. B. Schlegel, G. E. Scuseria, M. A. Robb, J. R. Cheeseman, J. A. Montgomery Jr., T. Vreven, K. N. Kudin, J. C. Burant, J. M. Millam, S. S. Iyengar, J. Tomasi, V. Barone, B. Mennucci, M. Cossi, G. Scalmani, N. Rega, G. A. Petersson, H. Nakatsuji, M. Hada, M. Ehara, K. Toyota, R. Fukuda, J. Hasegawa, M. Ishida, T. Nakajima, Y. Honda, O. Kitao, H. Nakai, M. Klene, X. Li, J. E.

Copyright © 2008 John Wiley & Sons, Ltd.

Knox, H. P. Hratchian, J. B. Cross, V. Bakken, C. Adamo, J. Jaramillo, R. Gomperts, R. E. Stratmann, O. Yazyev, A. J. Austin, R. Cammi, C. Pomelli, J. W. Ochterski, P. Y. Ayala, K. Morokuma, G. A. Voth, P. Salvador, J. J. Dannenberg, V. G. Zakrzewski, S. Dapprich, A. D. Daniels, M. C. Strain, O. Farkas, D. K. Malick, A. D. Rabuck, K. Raghavachari, J. B. Foresman, J. V. Ortiz, Q. Cui, A. G. Baboul, S. Clifford, J. Cioslowski, B. B. Stefanov, G. Liu, A. Liashenko, P. Piskorz, I. Komaromi, R. L. Martin, D. J. Fox, T. Keith, M. A. Al-Laham, C. Y. Peng, A. Nanayakkara, M. Challacombe, P. M. W. Gill, B. Johnson, W. Chen, M. W. Wong, C. Gonzalez, J. A. Pople, *Gaussian, Inc., Wallingford CT*, **2004**.

[51] R. F. W. Bader, P. M. Beddall, *J. Chem. Phys.* **1972**, *56*, 3320.

[52] R. F. W. Bader, *AIMPAC, Suite of Programs for the Theory of Atoms in Molecules*, McMaster University, Hamilton, Ontario, Canada, **1991**.

[53] S. Noury, X. Krokidis, F. Fuster, B. Silvi, *Comp. Chem.* **1999**, *23*, 597.

[54] J. M. L. Martin, C. Van Alsenoy, *GAR2PED*, University of Antwerp, The Netherlands, **1995**.

[55] R. Bukowski, W. Cencek, P. Jankowski, B. Jeziorski, M. Jeziorska, S. A. Kucharski, V. F. Lotrich, A. J. Misquitta, R. Moszyński, K. Patkowski, S. Podeszwa, S. Rybak, K. Szalewicz, H. L. Williams, R. J. Wheatley, P. E. S. Wormer, P. S. Żuchowski, *SAPT2006: An ab initio program for many-body symmetry-adapted perturbation theory calculations of intermolecular interaction energies. sequential and parallel versions, see http://www.physics.udel.edu/∼szalewic/SAPT/SAPT.html*

[56] M. W. Schmidt, K. K. Baldridge, J. A. Boatz, S. T. Elbert, M. S. Gordon, J. H. Jensen, S. Koseki, N. Matsunaga, K. A. Nguyen, S. J. Su, T. L. Windus, M. Dupuis, J. A. Montgomery, *J. Comp. Chem.* **1993**, *14*, 1347.

[57] N. C. Handy, A. J. Cohen, *J. Chem. Phys.* **2002**, *116*, 5411.

[58] N. Troullier, J. L. Martins, *Phys. Rev. B* **1991**, *43*, 1993.

[59] S. Nosé, *J. Chem. Phys.* **1984**, *81*, 511.

[60] W. G. Hoover, *Phys. Rev. A* **1985**, *31*, 1695.

[61] *CPMD Copyright IBM Corp. 1990–2004, Copyright MPI fuer Festkoerperforschung Stuttgart*, **1997–2001**.

[62] G. Bergerhoff, M. Berndt, K. Brandenburg, *J. Res. Natl. Inst. Stand. Technol.* **1996**, *101*, 221.

[63] W. Humphrey, A. Dalke, K. Schulten, *J. Mol. Graph.* **1996**, *14*, 33.

[64] N. S. P. Bhuvanesh, J. H. Reibenspies, *Acta Cryst. Sect. E* **2005**, *61*, o362.

[65] N. S. P. Bhuvanesh, Y. G. Zhang, P. L. Lee, J. H. Reibenspies, *J. Appl. Crystallogr.* **2005**, *38*, 632.

[66] C. S. Tautermann, A. E. Voegele, K. R. Liedl, *J. Chem. Phys.* **2004**, *120*, 631.

[67] F. Fuster, B. Silvi, *Theor. Chem. Acc.* **2000**, *104*, 13.

[68] M. E. Alikhani, F. Fuster, B. Silvi, *Struct. Chem.* **2005**, *16*, 203.

[69] S. Rybak, B. Jeziorski, K. Szalewicz, *J. Chem. Phys.* **1991**, *95*, 6576.

Copyright © 2008 John Wiley & Sons, Ltd.